

Article

A Giant Truncated Metallo-tetrahedron with Unexpected Supramolecular Aggregation Induced Emission Enhancement

Die Liu, Mingzhao Chen, Kaixiu Li, Zhengguang Li, Jian Huang, Jun Wang, Zhilong Jiang, Zhe Zhang, Tingzheng Xie, George R. Newkome, and Pingshan Wang

J. Am. Chem. Soc., **Just Accepted Manuscript** • DOI: 10.1021/jacs.0c02366 • Publication Date (Web): 10 Apr 2020

Downloaded from pubs.acs.org on April 13, 2020

Just Accepted

“Just Accepted” manuscripts have been peer-reviewed and accepted for publication. They are posted online prior to technical editing, formatting for publication and author proofing. The American Chemical Society provides “Just Accepted” as a service to the research community to expedite the dissemination of scientific material as soon as possible after acceptance. “Just Accepted” manuscripts appear in full in PDF format accompanied by an HTML abstract. “Just Accepted” manuscripts have been fully peer reviewed, but should not be considered the official version of record. They are citable by the Digital Object Identifier (DOI®). “Just Accepted” is an optional service offered to authors. Therefore, the “Just Accepted” Web site may not include all articles that will be published in the journal. After a manuscript is technically edited and formatted, it will be removed from the “Just Accepted” Web site and published as an ASAP article. Note that technical editing may introduce minor changes to the manuscript text and/or graphics which could affect content, and all legal disclaimers and ethical guidelines that apply to the journal pertain. ACS cannot be held responsible for errors or consequences arising from the use of information contained in these “Just Accepted” manuscripts.

A Giant Truncated Metallo-tetrahedron with Unexpected Supramolecular Aggregation Induced Emission Enhancement

Die Liu,[†] Mingzhao Chen,[†] Kaixiu Li,[‡] Zhengguang Li,[‡] Jian Huang,[‡] Jun Wang,[‡] Zhilong Jiang,[†] Zhe Zhang,[†] Tingzheng Xie,[†] George R. Newkome,[¶] Pingshan Wang^{†,‡,*}

[†]Institute of Environmental Research at Greater Bay Area; Key Laboratory for Water Quality and Conservation of the Pearl River Delta, Ministry of Education; Guangzhou Key Laboratory for Clean Energy and Materials, Guangzhou University, Guangzhou-510006, China

[‡]Hunan Key Laboratory of Micro & Nano Materials Interface Science; College of Chemistry and Chemical Engineering, Central South University, Changsha, Hunan-410083, China

[¶]Center for Molecular Biology and Biotechnology, Florida Atlantic University, 5353 Parkside Dr., Jupiter, FL-33458, USA

Self-Assembly • Aggregation Induced Emission • Multitopic Terpyridine Ligands • Spoked Wheels

ABSTRACT: The artificial synthesis of giant, three-dimensional and shell-like architectures with growing complexity and novel functionalities is an especially challenging task for chemists. Fullerenes and self-assembled cages are remarkable examples that are proved milestones in the field of functional materials. Herein, we present another unique system: a giant terpyridine-based truncated metallo-tetrahedral architecture that includes dense-packed ionic pairs with a significant internal cavity. This huge metallo-tetrahedron with a molecular weight up to 70,000 Da was self-assembled simultaneously with 64 components: 12 large antler-shaped ligands (5), 4 star-shaped ligands (6) and 48 Cd²⁺ ions. Surprisingly, the giant tetrahedron shows broad visible emission (400–640 nm) and the aggregation induced emission enhancement (AIEE) via hierarchical assembly into highly ordered nano-aggregates. Tunable emission color and near white-light emission in mixed solvent systems were also achieved. The present work not only affords an effective approach to the creation of giant shell-like architectures that can be used to mimic biological viruses and chemical frameworks but also provides a new class of functional metallo-architectures.

INTRODUCTION

Supramolecular polyhedral assemblies are quite fascinating not only because of their aesthetically appealing structures, but also due to their broad applications ranging from catalysis,^{1–2} sensing,^{3–5} drug delivery,^{6–8} separation and purify,^{9–12} to photophysical applications.¹³ The most common and important kind of these architectures were ones constructed by the coordination-driven self-assembly, which possess the highly directional and predictable feature to attain the desirable structure with precise shapes and sizes. And a great amount of excellent work, including tetrahedra,^{14–19} cubes,^{20, 21} octahedra,²² cuboctahedra,^{23–25} dodecahedra,²⁶ and others,^{2, 27–38} has been well demonstrated by Stoddart, Stang, Fujita, Leigh, Nitschke, Newkome, and many others.

Several fascinating metallocages with various sizes, shapes and functionality have been shown, but the giant, complicated polyhedral structures assembled by more than 60 components are uncommon due to the difficulty associated with ligand design and assembly process.^{39–42} Despite these challenges, using chemical synthetic strategy to create such multicomponent supramolecules to mimic natural biological structures is still meaningful. For

example, Nitschke's group synthesized a huge Co^{II}₁₂L₆ cuboctahedron, which was capable of cooperatively binding anionic and neutral guests. Further, the bis-fullerene receptor showed different cooperativity in binding pairs of anions, which make it fit to construct the programmable molecular systems. Fujita et al synthesized the self-assembled Pd^{II}₁₂L₂₄ cage-like host with large size, which was able to encapsulate the protein and such work lay the foundation for regulating the conformation and functionality of protein.⁴³

Recently, the coordination-driven supramolecular cages with aggregation-induced emission (AIE)^{44, 45} property and their fascinating optical properties have drawn intense attention.^{46–53} Among these architectures, the most were generated by incorporating the tetraphenylethylene (TPE) moieties to molecular scaffolds. For example, Stang and co-workers synthesized the pyridine-based M₁₂L₂₄ nanospheres, which were covalently *endo*-anchored with TPE moieties, displaying the stronger green light emission in solution due to AIE effect on confined cavity.⁵¹ But the cages without TPE moieties, yet possessing AIE effect, have rarely been reported.⁵⁰

2,2':6',2''-terpyridine (tpy) ligands could coordinate with transition metal ions to generate linear <tpy-M-tpy>

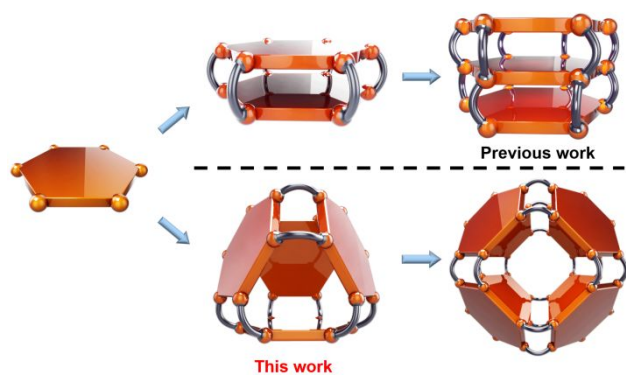


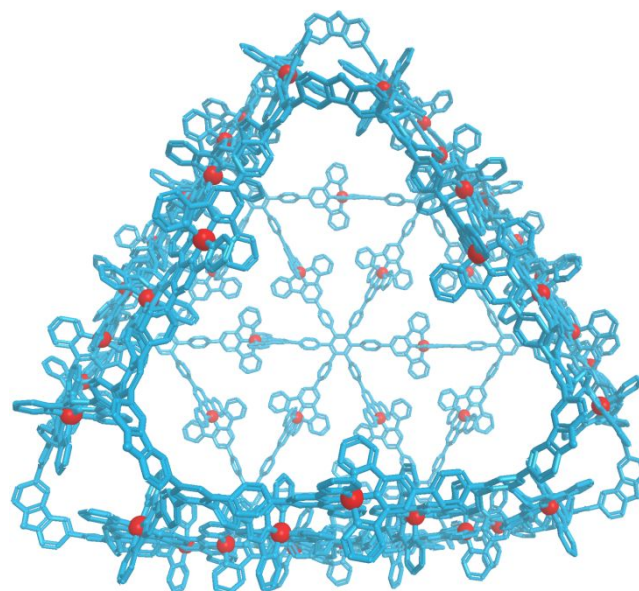
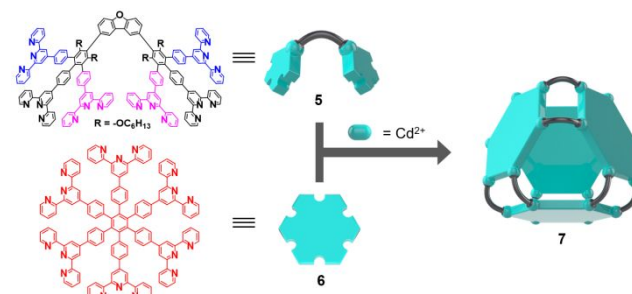
Figure 1. Cartoon representation of vertical assembly of double- and triple-decker hexagonal architectures and polyhedral assembly of tetrahedron and octahedron from the spoked wheel-like hexagon.

pseudooctahedral coordination connection and were ideal candidates to construct 2D/3D self-assembled architectures.^{54, 55} As shown in Scheme S1, the giant 2D shape-persistent spoked wheel hexagons, firstly synthesized by Newkome *et al.*, were demonstrated to be incredibly stable.⁵⁶ So the hexagon is especially suitable as a plane unit to construct complicated 3D structures. Surely, as shown in Figure 1 and Scheme 1, by connecting the spoked wheels with flexible alkyl linkers, the double- and triple-decker hexagons were successfully synthesized via the vertically extending the plane spoked wheels by our group.⁵⁷ But such strategy lead to the absence of cavities for resultant assemblies and limited structural diversity. As shown in Scheme 1, if using ligands with different, tailored angles to install the directed rigid bridge to connect hexagonal moieties, the cavities-containing polyhedrons, including truncated tetrahedra, truncated octahedra and truncated icosahedra, could be obtained in theory. In this paper, we synthesized the dibenzo[*b,d*]furan bridged ligands **5** containing two 2,8-position substitutional tristerpyridines. Such ligands **5** (12 eq.) could assemble with **6** (4 eq.) and Cd²⁺ (48 eq.) to generate a giant cage-like truncated tetrahedron, which consist of 64 components and whose molecule weight up to 70 kDa. Unexpectedly, this 3D supramolecular structure displayed the unusual and appealing aggregation induced emission enhancement (AIEE) effect.

RESULTS AND DISCUSSION

As shown in Scheme 1 and Scheme S2, ligand **5** was designed and synthesized by Suzuki coupling of the bromo-substituted tristerpyridine monomer **4** with 2,8-bis(4,4,5,5-tetramethyl-1,3,2-dioxaborolan-2-yl) dibenzo[*b,d*]furan catalyzed by [Pd(PPh₃)₄]. Purification was accomplished by column chromatography (Al₂O₃) and subsequent recrystallization with CH₂Cl₂ and MeOH. ¹H NMR of **5** showed two set of peaks with 1:2 integrated ratio attributed to two different terpyridinyl moieties, along with a triplet at 3.12 ppm assigned to the methylene groups. Structural characterization of **5** was further supported by MALDI-TOF-MS analysis (Figure S13).

Scheme 1. Self-assembly and energy-minimized structures from molecular modeling of complex **7** (the alkyl chains are omitted for clarity).



As shown in Scheme 1, the self-assembly process began by mixing **5** (3 eq.), **6** (1 eq.) and Cd(NO₃)₂·4H₂O (12 eq.) in CHCl₃/MeOH at 65 °C for 24 h, yielding a translucent colourless solution. Excess lithium bis(trifluoromethylsulfonyl)imide (LiNTf₂) was then added to give a precipitate, which was washed with MeOH and H₂O to generate (92%) complex **7**, as a pale-yellow solid.

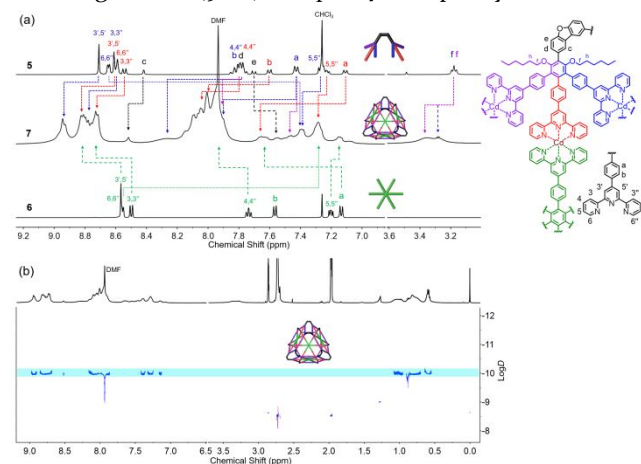


Figure 2. (a) ¹H NMR spectra (500 MHz) of ligand **5** and **6** in CDCl₃ and complex **7** in CD₃CN/[D₇]DMF (4:1, v/v) and (b) 2D DOSY NMR spectra of complex **7** (500 MHz, CD₃CN/[D₇]DMF (4:1, v/v), 300 K).

Although the self-assembled complex **7** was a large supramolecular architecture, its ^1H NMR spectrum showed a broad but yet distinguishable pattern. Firstly, when comparing free ligand **5** and **6**, the signals of $\text{tpyH}^{3,5'}$ and $\text{tpyH}^{3,3'}$ protons (Figure 2a) showed obvious downfield shifts caused by the tangential electron-withdrawing effects upon coordination. The $\text{tpyH}^{6,6'}$ protons displayed a dramatic up-field shift due to the electron shielding effect.⁵⁰ These signal changes demonstrated that the assembled structure was generated. Furthermore, the triplet at 3.12 ppm, assigned to methylene groups, split into two peaks at 3.28 ppm and 3.32 ppm because of that the free rotation of *tris*-terpyridine moieties was restricted and the symmetry of **5** was broken, fully supporting the formation of polyhedral structure. All of signals of protons could be assigned by means of the 2D-COSY and NOESY NMR.

Diffusion-ordered NMR spectroscopy (DOSY) spectrum of tetrahedral complex **7** (Figure 2b) showed that the protons signals of tetrahedral structure were on a narrow band with $\log D = -9.96$, supporting the formation of a single discrete structure. The dynamic radius was calculated by Stokes-Einstein equation to be 5.4 nm, which was in accord with the energy-minimized tetrahedron structure, verifying the formation of cage-like tetrahedron structure. In addition, the signal corresponding to the solvent DMF showed a series of continuous signals for complex **7**, indicating the cage-like complex **7** possessed a large cavity and could encapsulate the DMF molecules in order to restrict their free diffusion.

The ESI mass spectrum of **7** (Figure 3a) validated the expected 64-component composition of $[\text{5}_{12}\text{6}_4\text{Cd}_{48}]$, in which a series of peaks corresponding to sequential charge states ranging from 16^+ to 32^+ were observed. The molecular weight was 70759.78 Da, consistent with the molecular formula of $[\text{Cd}_{48}(\text{C}_{2616}\text{H}_{2040}\text{N}_{288}\text{O}_{60})]^{96+}\cdot 96(\text{NTf}_2^-)$. Although the isotope pattern of each charge state in the mass measurements was indistinct resulting from high molecular weight and the giant cavity which encapsulated the solvent molecules, this set of distinct signals presented a perfect

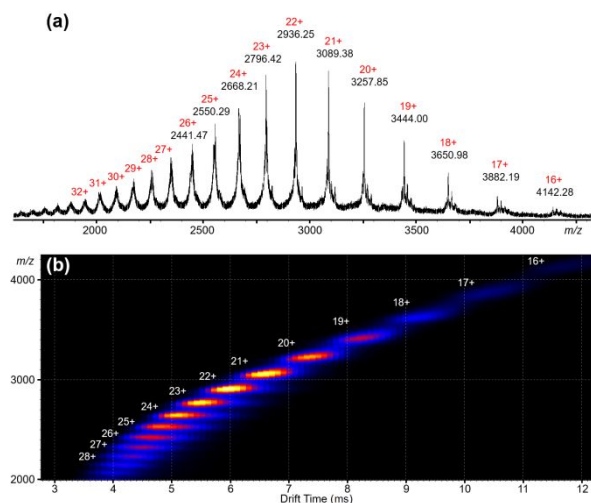


Figure 3. (a) ESI-MS and (b) 2D ESITWIM-MS plot (m/z vs drift time) of complex **7**. The charge states of intact assemblies are marked.

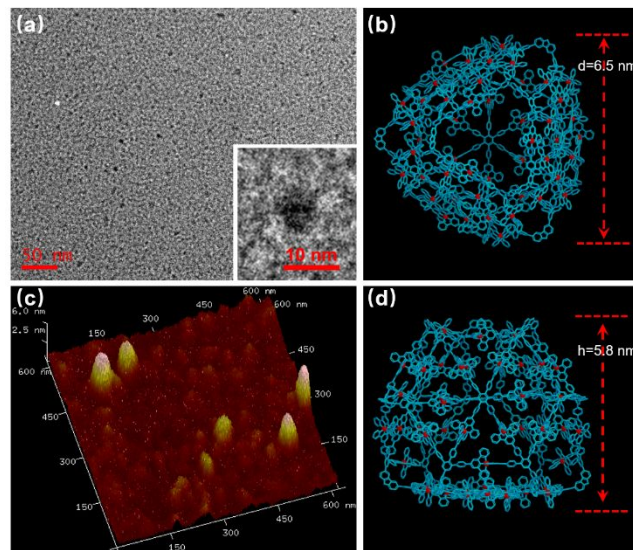


Figure 4. (a) TEM image; (b) representative energy-minimized structure, at top view; (c) AFM image and (d) a side view of the energy-minimized structure of tetrahedral structure **7**.

match with the simulated m/z verifying the desired truncated tetrahedral structure. Additional structural evidence for complex **7** was provided by ESI-TWIM MS experiments. The TWIM mass spectrum exhibited continuous charge distributions ranging from 16^+ to 30^+ derived from **7**, with a single band for every signal, supporting the presence of a single species (Figure 3b).

Structural evidences were further obtained by the TEM and AFM experiments. As depicted in Figures 4a and S18, TEM images determined by drop casting of dilute acetonitrile solutions of complex **7** (10^{-6} – 10^{-7} M) onto carbon film-coated Cu grid displayed the uniform particle with an average diameter of 6.2 nm, which was in accordance with the size of molecular modeling (6.5 nm, Figure 4b). The AFM images (Figures 4c and S19) obtained by dropping acetonitrile solutions (10^{-6} – 10^{-7} M)

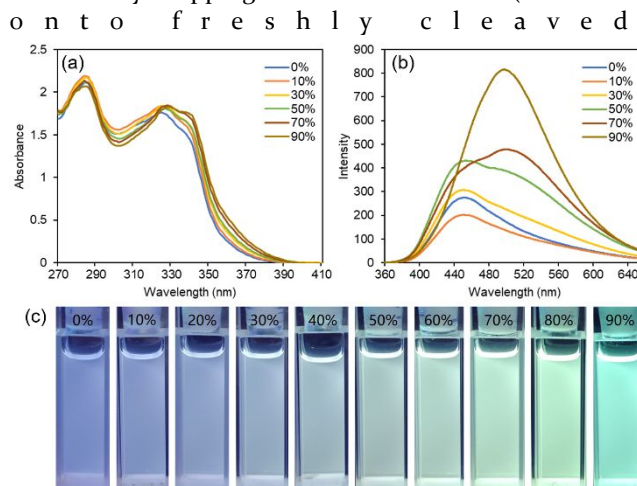


Figure 5. (a) UV/Vis absorption spectra, (b) fluorescence spectra ($\lambda_{\text{ex}} = 340 \text{ nm}$, $c = 7 \times 10^{-7} \text{ M}$), and (c) photographs ($\lambda_{\text{ex}} = 365 \text{ nm}$, $c = 7 \times 10^{-7} \text{ M}$) of complex **7** in DMF (1%, v/v)/MeCN mixture with adding various CHCl_3 fractions.

mica showed average height of 6.4 nm, which agreed with the calculated height of model structure of 5.8 nm (Figure 4d).

Based on previous data, the tpy-based complexes possessed excellent emission properties.⁵⁸ The giant tetrahedral **7**, which possess 48 <tpy-Cd²⁺-tpy> moieties (96 positive charges), was characterized by UV-Vis absorption and fluorescence experiments to evaluate its optical properties. The UV-vis absorption spectrum in MeCN:DMF ($7 \times 10^{-7} \text{ M}$, 99:1, v/v) at 25 °C exhibited a distinct band with high molar extinction coefficient at 285 nm assigned to ligand-centered (LC) $\pi-\pi^*$ transitions and the band centered at ~ 325 with the shoulder at ~ 337 nm (Figure 5a), was attributed to intraligand charge transfer (ILCT).^{59, 60} The emission spectrum of complex **7** in a MeCN/DMF (99/1 in v/v) solution showed two broad bands centered at 440 and 500 nm (Figure 5b), which could be presumably assigned to the $\pi-\pi^*$ and ILCT states^{59, 60} and almost covered the entire visible spectral region (400–640nm).

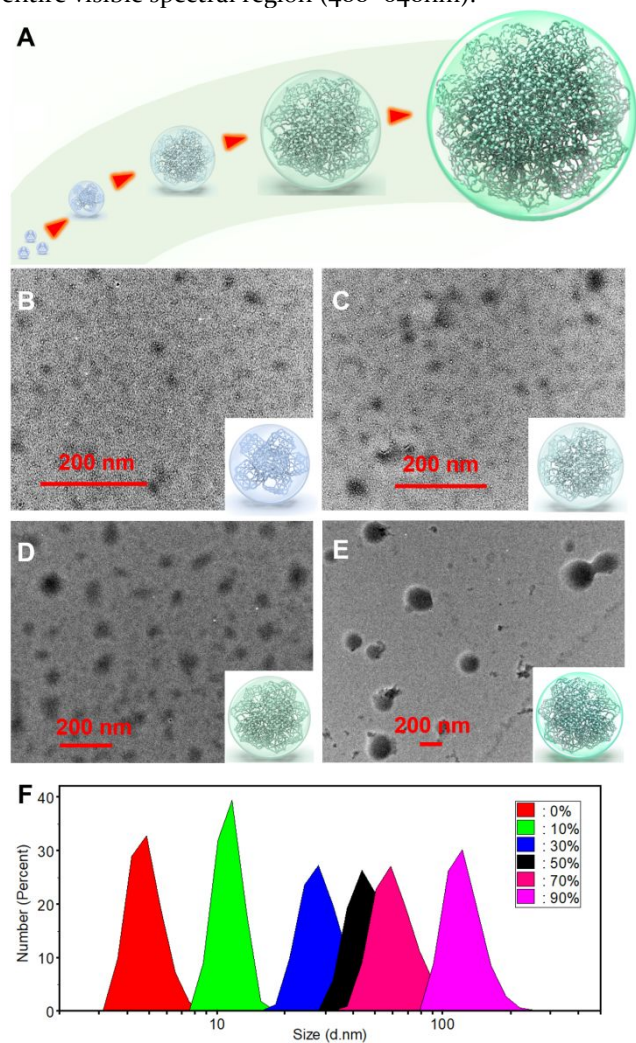


Figure 6. TEM images of complex **7** in DMF (1%, v/v)/CH₃CN mixture with various CHCl₃ fractions and corresponding schematic illustration of aggregates: (a) schematic representation of aggregates forming, (b) 30%. (c) 50%. (d) 70%. (e) 90%. (scale bar: 200 nm) And (f) DLS datum.

More fascinating, complex **7** exhibited aggregation induced emission enhancement (AIEE), in which the fluorescence intensity showed an obvious increment into 1.7, 3.2, 1.6, 1.1 and 4.6 times in the mixture with 95% poor solvent corresponding to CH₂Cl₂, CHCl₃, EtOAc, MeOH, and H₂O, respectively (Figure S31). The emission behavior of complex **7** was further investigated in mixed systems with different CHCl₃ (or CH₂Cl₂) fractions. As shown in Figures 5b, S31 and S33, the intensity of the band around *ca.* 500 nm was clearly enhanced and the band at *ca.* 440 nm slightly enhanced by increasing the fraction of CHCl₃ (or CH₂Cl₂) from 10 to 90%. Accordingly, the emission color changed from cyan to green for CHCl₃ (Figure 5c) and to yellow-green for CH₂Cl₂ (Figure S34) and the near white light emission with coordination (0.2444, 0.3358) in the Commission Internationale de L'Eclairage (CIE) chromaticity diagram could be achieved (Figures S33 and S35). In contrast, the emission intensity of ligand **5** and **6** showed a clear decrease due to aggregation, followed by increasing the MeOH fraction from 10% to 90% in CHCl₃/MeOH mixture (Figure S30). The decreased emission of **5** and **6** resulted from an aggregation-caused quench (ACQ) effect, in which the $\pi-\pi$ stacking of rigid π conjugated **5** and **6** was easily formed via the compact aggregations (Figure S27).^{61, 62} However, $\pi-\pi$ stacking induced emission quench under aggregation is the unfavorable result of the 3D configuration and ion pair steric hindrance of this cage-like structure **7**. We speculate that the enhanced emission of complex **7** resulted from the AIE behavior, in which the aggregation formed in a poor solvent mixture (with higher CHCl₃ concentration) restricted intramolecular rotation (RIR) of the aromatic rings.^{50, 63, 64} For the purpose of obtaining more evidence of the aggregation, a series of UV-vis spectra were recorded in a MeCN/CHCl₃ system with the different fraction of poor solvent *e.g.*, CHCl₃, from 10 to 90%. As shown in Figures 5a and S28, the band at 285 nm decreased, with a coincidental enhancement of absorbance at 370–400 nm, demonstrating that complexes **7** were brought into close proximity and formed aggregates.⁶⁵

The sequentially aggregating in a poor solvent mixture was schematically illustrated in Figure 6a. TEM and AFM experiments afforded direct evidence for the formation of aggregates. As displayed in Figures 6b–e and Figures S20–26, the images determined by drop-casting the mixture onto a Cu grid for TEM or mica sheet for AFM showed that the nanospherical particles formed in the DMF/CH₃CN/CHCl₃ mixture. And the size of the aggregates increased as the CHCl₃ fraction increasing; the average diameter of aggregates reached 185 nm from the TEM images after adding 90% CHCl₃. The size, determined by TEM and AFM experiments, was obviously larger than the results from DLS experiments, indicating that the aggregates were unstable and easily collapsed to form

oblate structure on a solid surface. In order to obtain the evidence for the aggregation behaviors, the dynamic light scattering (DLS) experiments were performed in a mixed DMF/MeCN/CHCl₃ solvent. The results were shown in Figure 6f, in which the average hydrodynamic diameters (D_h) of **7** was determined to 5.6 nm in DMF/MeCN without CHCl₃, indicating no aggregation. However, the D_h continuously changed from 12 to 147 nm with increasing CHCl₃ fractions from 10% to 90%, demonstrating that the higher-order nano-aggregates were generated in the DMF/MeCN/CHCl₃ system.

CONCLUSIONS

In conclusion, the giant truncated tetrahedron **7** with the molecular weight up to 70,000 Da was nearly qualitatively synthesized via a one-pot self-assembly of 64 components. The composition and structure were characterized by a combination of ¹H NMR, DOSY NMR, DLS, ESI-MS, TWIM-MS, TEM and AFM images. More importantly, the multicharged metal-organic complex **7** was able to further self-assemble into highly ordered nano-aggregates and showed that the aggregation-induced emission enhancement, along with tunable emission color and near white-light emission in mixed solvent systems. This research provides new insight into optically-active metallo-supramolecules obtained by a simple, one-step rational design.

ASSOCIATED CONTENT

The Supporting Information is available free of charge on the ACS Publications website at <http://pubs.acs.org> at DOI: 10.1021/. Experimental procedures and characterization data, including ¹H, ¹³C, COSY, NOESY, and DOSY spectra of the new compounds and ESI-MS spectra, TEM and AFM images of related compounds (PDF)

AUTHOR INFORMATION

Corresponding Author

*P. Wang: chemwps@csu.edu.cn.

ORCID

Pingshan Wang: 0000-0002-1988-7604.

Die Liu: 0000-0002-3918-0569.

Notes

The authors declare no competing financial interest.

ACKNOWLEDGMENT

This research was supported by the National Natural Science Foundation of China (21971257) and the Hunan Provincial Science and Technology Plan Project of China (No. 2019TP1001) for P.W., the Natural Science Foundation of Guangdong Province, China (No. 2019A151501358) for Z. Z.. The authors grateful acknowledge Prof. Dr. Carol D. Kercher for her professional consultation.

REFERENCES

1. Bender, T. A.; Bergman, R. G.; Raymond, K. N.; Toste, F. D., A Supramolecular Strategy for Selective Catalytic

Hydrogenation Independent of Remote Chain Length. *J. Am. Chem. Soc.* **2019**, *141*, 11806-11810.

2. Wei, J.; Zhao, L.; He, C.; Zheng, S.; Reek, J. N. H.; Duan, C., Metal-Organic Capsules with NADH Mimics as Switchable Selectivity Regulators for Photocatalytic Transfer Hydrogenation. *J. Am. Chem. Soc.* **2019**, *141*, 12707-12716.

3. Bravin, C.; Mason, G.; Licini, G.; Zonta, C., A Diastereodynamic Probe Transducing Molecular Length into Chiroptical Readout. *J. Am. Chem. Soc.* **2019**, *141*, 11963-11969.

4. Bravin, C.; Guidetti, A.; Licini, G.; Zonta, C., Supramolecular cages as differential sensors for dicarboxylate anions: guest length sensing using principal component analysis of ESI-MS and ¹H-NMR raw data. *Chem. Sci.* **2019**, *10*, 3523-3528.

5. Jiang, X.-F.; Hau, F. K.-W.; Sun, Q.-F.; Yu, S.-Y.; Yam, V. W.-W., From {Au^I...Au^I}-Coupled Cages to the Cage-Built 2-D {Au^I...Au^I} Arrays: Au^I...Au^I Bonding Interaction Driven Self-Assembly and Their Ag^I Sensing and Photo-Switchable Behavior. *J. Am. Chem. Soc.* **2014**, *136*, 10921-10929.

6. Lewis, J. E. M.; Gavey, E. L.; Cameron, S. A.; Crowley, J. D., Stimuli-responsive Pd₂L₄ metallocupramolecular cages: towards targeted cisplatin drug delivery. *Chem. Sci.* **2012**, *3*, 778-784.

7. Schmidt, A.; Casini, A.; Kühn, F. E., Self-assembled M₂L₄ coordination cages: Synthesis and potential applications. *Coord. Chem. Rev.* **2014**, *275*, 19-36.

8. Han, J.; Schmidt, A.; Zhang, T.; Permentier, H.; Groothuis, G. M. M.; Bischoff, R.; Kühn, F. E.; Horvatovich, P.; Casini, A., Bioconjugation strategies to couple supramolecular exo-functionalized palladium cages to peptides for biomedical applications. *Chem. Commun.* **2017**, *53*, 1405-1408.

9. Pan, M.; Wu, K.; Zhang, J.-H.; Su, C.-Y., Chiral metal-organic cages/containers (MOCs): From structural and stereochemical design to applications. *Coord. Chem. Rev.* **2019**, *378*, 333-349.

10. Liu, J.; Duan, W.; Song, J.; Guo, X.; Wang, Z.; Shi, X.; Liang, J.; Wang, J.; Cheng, P.; Chen, Y.; Zaworotko, M. J.; Zhang, Z., Self-Healing Hyper-Cross-Linked Metal-Organic Polyhedra (HCMOPs) Membranes with Antimicrobial Activity and Highly Selective Separation Properties. *J. Am. Chem. Soc.* **2019**, *141*, 12064-12070.

11. Zhang, H.-N.; Lu, Y.; Gao, W.-X.; Lin, Y.-J.; Jin, G.-X., Selective Encapsulation and Separation of Dihalobenzene Isomers with Discrete Heterometallic Macrocages. *Chem. - Eur. J.* **2018**, *24*, 18913-18921.

12. Kieffer, M.; Garcia, A. M.; Haynes, C. J. E.; Kralj, S.; Iglesias, D.; Nitschke, J. R.; Marchesan, S., Embedding and Positioning of Two Fe^{II}₄L₄ Cages in Supramolecular Tripeptide Gels for Selective Chemical Segregation. *Angew. Chem. Int. Ed.* **2019**, *58*, 7982-7986.

13. Saha, M. L.; Yan, X.; Stang, P. J., Photophysical Properties of Organoplatinum(II) Compounds and Derived Self-Assembled Metallacycles and Metallacages: Fluorescence and its Applications. *Acc. Chem. Res.* **2016**, *49*, 2527-2539.

14. Kaphan, D. M.; Levin, M. D.; Bergman, R. G.; Raymond, K. N.; Toste, F. D., A supramolecular microenvironment strategy for transition metal catalysis. *Science* **2015**, *350*, 1235-1238.

15. MacGillivray, L. R.; Atwood, J. L., A chiral spherical molecular assembly held together by 60 hydrogen bonds. *Nature* **1997**, *389*, 469-472.

16. Roberts, D. A.; Pilgrim, B. S.; Cooper, J. D.; Ronson, T. K.; Zarra, S.; Nitschke, J. R., Post-assembly Modification of Tetrazine-Edged Fe^{II}₄L₆ Tetrahedra. *J. Am. Chem. Soc.* **2015**, *137*, 10068-10071.

17. Cao, L.; Wang, P.; Miao, X.; Dong, Y.; Wang, H.; Duan, H.; Yu, Y.; Li, X.; Stang, P. J., Diamondoid Supramolecular Coordination Frameworks from Discrete Adamantanoid Platinum(II) Cages. *J. Am. Chem. Soc.* **2018**, *140*, 7005-7011.

18. Mahata, K.; Frischmann, P. D.; Würthner, F., Giant Electroactive M_4L_6 Tetrahedral Host Self-Assembled with Fe(II) Vertices and Perylene Bisimide Dye Edges. *J. Am. Chem. Soc.* **2013**, *135*, 15656-15661.
19. Hong, C. M.; Morimoto, M.; Kapustin, E. A.; Alzakhem, N.; Bergman, R. G.; Raymond, K. N.; Toste, F. D., Deconvoluting the Role of Charge in a Supramolecular Catalyst. *J. Am. Chem. Soc.* **2018**, *140*, 6591-6595.
20. Suzuki, K.; Tominaga, M.; Kawano, M.; Fujita, M., Self-assembly of an M_6L_{12} coordination cube. *Chem. Commun.* **2009**, 1638-1640.
21. Meng, W.; Breiner, B.; Rissanen, K.; Thoburn, J. D.; Clegg, J. K.; Nitschke, J. R., A Self-Assembled M_8L_6 Cubic Cage that Selectively Encapsulates Large Aromatic Guests. *Angew. Chem. Int. Ed.* **2011**, *50*, 3479-3483.
22. Tan, C.; Jiao, J.; Li, Z.; Liu, Y.; Han, X.; Cui, Y., Design and Assembly of a Chiral Metallosalen-Based Octahedral Coordination Cage for Supramolecular Asymmetric Catalysis. *Angew. Chem. Int. Ed.* **2018**, *57*, 2085-2090.
23. Clingerman, D. J.; Kennedy, R. D.; Mondloch, J. E.; Sarjeant, A. A.; Hupp, J. T.; Farha, O. K.; Mirkin, C. A., An exceptionally high boron content supramolecular cuboctahedron. *Chem. Commun.* **2013**, *49*, 11485-11487.
24. Ghosh, K.; Hu, J.; White, H. S.; Stang, P. J., Construction of Multifunctional Cuboctahedra via Coordination-Driven Self-Assembly. *J. Am. Chem. Soc.* **2009**, *131*, 6695-6697.
25. Xie, T.-Z.; Guo, K.; Guo, Z.; Gao, W.-Y.; Wojtas, L.; Ning, G.-H.; Huang, M.; Lu, X.; Li, J.-Y.; Liao, S.-Y.; Chen, Y.-S.; Moorefield, C. N.; Saunders, M. J.; Cheng, S. Z. D.; Wesdemiotis, C.; Newkome, G. R., Precise Molecular Fission and Fusion: Quantitative Self-Assembly and Chemistry of a Metallo-Cuboctahedron. *Angew. Chem. Int. Ed.* **2015**, *54*, 9224-9229.
26. Olenyuk, B.; Levin, M. D.; Whiteford, J. A.; Shield, J. E.; Stang, P. J., Self-Assembly of Nanoscopic Dodecahedra from 50 PreDesigned Components. *J. Am. Chem. Soc.* **1999**, *121*, 10434-10435.
27. Guo, B. C.; Kerns, K. P.; Jr, C. A., Ti_8C^{12+} -Metallo-Carbohedrenes: A New Class of Molecular Clusters? *Science* **1992**, *255*, 1411-1413.
28. Yamashina, M.; Akita, M.; Hasegawa, T.; Hayashi, S.; Yoshizawa, M., A polyaromatic nanocapsule as a sucrose receptor in water. *Sci. Adv.* **2017**, *3*, e1701126.
29. Yamashina, M.; Tanaka, Y.; Lavendomme, R.; Ronson, T. K.; Pittelkow, M.; Nitschke, J. R., An antiaromatic-walled nanospace. *Nature* **2019**, *574*, 511-515.
30. Li, X.-Z.; Zhou, L.-P.; Yan, L.-L.; Yuan, D.-Q.; Lin, C.-S.; Sun, Q.-F., Evolution of Luminescent Supramolecular Lanthanide $M_{2n}L_{3n}$ Complexes from Helicates and Tetrahedra to Cubes. *J. Am. Chem. Soc.* **2017**, *139*, 8237-8244.
31. Wu, K.; Li, K.; Hou, Y.-J.; Pan, M.; Zhang, L.-Y.; Chen, L.; Su, C.-Y., Homochiral D₄-symmetric metal-organic cages from stereogenic Ru(II) metalloligands for effective enantioseparation of atropisomeric molecules. *Nat. Commun.* **2016**, *7*, 10487.
32. Bloch, W. M.; Abe, Y.; Holstein, J. J.; Wandtke, C. M.; Dittrich, B.; Clever, G. H., Geometric Complementarity in Assembly and Guest Recognition of a Bent Heteroleptic cis-[Pd₂LA₂LB₂] Coordination Cage. *J. Am. Chem. Soc.* **2016**, *138*, 13750-13755.
33. Zhang, X.; Dong, X.; Lu, W.; Luo, D.; Zhu, X.-W.; Li, X.; Zhou, X.-P.; Li, D., Fine-Tuning Apertures of Metal-Organic Cages: Encapsulation of Carbon Dioxide in Solution and Solid State. *J. Am. Chem. Soc.* **2019**, *141*, 11621-11627.
34. Cetin, M. M.; Beldjoudi, Y.; Roy, I.; Anamimoghadam, O.; Bae, Y. J.; Young, R. M.; Krzyaniak, M. D.; Stern, C. L.; Philp, D.; Alsubaie, F. M.; Wasielewski, M. R.; Stoddart, J. F., Combining Intra- and Intermolecular Charge Transfer with Polycationic Cyclophanes To Design 2D Tessellations. *J. Am. Chem. Soc.* **2019**, *141*, 18727-18739.
35. Shen, D.; Cooper, J. A.; Li, P.; Guo, Q.-H.; Cai, K.; Wang, X.; Wu, H.; Chen, H.; Zhang, L.; Jiao, Y.; Qiu, Y.; Stern, C. L.; Liu, Z.; Sue, A. C. H.; Yang, Y.-W.; Alsubaie, F. M.; Farha, O. K.; Stoddart, J. F., Organic Counteranion Co-assembly Strategy for the Formation of γ -Cyclodextrin-Containing Hybrid Frameworks. *J. Am. Chem. Soc.* **2020**, *142*, 2042-2050.
36. Li, P.; Chen, Z.; Ryder, M. R.; Stern, C. L.; Guo, Q.-H.; Wang, X.; Farha, O. K.; Stoddart, J. F., Assembly of a Porous Supramolecular Polyknot from Rigid Trigonal Prismatic Building Blocks. *J. Am. Chem. Soc.* **2019**, *141*, 12998-13002.
37. Leigh, D. A.; Pirvu, L.; Schaufelberger, F.; Tetlow, D. J.; Zhang, L., Securing a Supramolecular Architecture by Tying a Stopper Knot. *Angew. Chem. Int. Ed.* **2018**, *57*, 10484-10488.
38. Zhang, L.; Marcos, V.; Leigh, D. A., Molecular machines with bio-inspired mechanisms. *Proc. Natl. Acad. Sci. USA* **2018**, *115*, 9397-9404.
39. Fujita, D.; Ueda, Y.; Sato, S.; Yokoyama, H.; Mizuno, N.; Kumasaka, T.; Fujita, M., Self-Assembly of $M_{30}L_{60}$ Icosidodecahedron. *Chem* **2016**, *1*, 91-101.
40. Fujita, D.; Ueda, Y.; Sato, S.; Mizuno, N.; Kumasaka, T.; Fujita, M., Self-assembly of tetravalent Goldberg polyhedra from 144 small components. *Nature* **2016**, *540*, 563.
41. Zhou, X.-P.; Liu, J.; Zhan, S.-Z.; Yang, J.-R.; Li, D.; Ng, K.-M.; Sun, R. W.-Y.; Che, C.-M., A High-Symmetry Coordination Cage from 38- or 62-Component Self-Assembly. *J. Am. Chem. Soc.* **2012**, *134*, 8042-8045.
42. Rizzuto, F. J.; Nitschke, J. R., Stereochemical plasticity modulates cooperative binding in a $Co_{11}L_{12}L_6$ cuboctahedron. *Nat. Chem.* **2017**, *9*, 903-908.
43. Fujita, D.; Suzuki, K.; Sato, S.; Yagi-Utsumi, M.; Yamaguchi, Y.; Mizuno, N.; Kumasaka, T.; Takata, M.; Noda, M.; Uchiyama, S.; Kato, K.; Fujita, M., Protein encapsulation within synthetic molecular hosts. *Nat. Commun.* **2012**, *3*, 1093.
44. Luo, J.; Xie, Z.; Lam, J. W. Y.; Cheng, L.; Chen, H.; Qiu, C.; Kwok, H. S.; Zhan, X.; Liu, Y.; Zhu, D.; Tang, B. Z., Aggregation-induced emission of 1-methyl-1,2,3,4,5-pentaphenylsilole. *Chem. Commun.* **2001**, 1740-1741.
45. Feng, H.-T.; Lam, J. W. Y.; Tang, B. Z., Self-assembly of AIEgens. *Coord. Chem. Rev.* **2020**, *406*, 213142.
46. Yu, G.; Cook, T. R.; Li, Y.; Yan, X.; Wu, D.; Shao, L.; Shen, J.; Tang, G.; Huang, F.; Chen, X.; Stang, P. J., Tetraphenylethene-based highly emissive metallacage as a component of theranostic supramolecular nanoparticles. *Proc. Natl. Acad. Sci. USA* **2016**, *113*, 13720-13725.
47. Yan, X.; Cook, T. R.; Wang, P.; Huang, F.; Stang, P. J., Highly emissive platinum(II) metallacages. *Nat. Chem.* **2015**, *7*, 342.
48. Wang, M.; Zheng, Y.-R.; Ghosh, K.; Stang, P. J., Metallocsupramolecular Tetragonal Prisms via Multicomponent Coordination-Driven Template-Free Self-Assembly. *J. Am. Chem. Soc.* **2010**, *132*, 6282-6283.
49. Zhang, M.; Saha, M. L.; Wang, M.; Zhou, Z.; Song, B.; Lu, C.; Yan, X.; Li, X.; Huang, F.; Yin, S.; Stang, P. J., Multicomponent Platinum(II) Cages with Tunable Emission and Amino Acid Sensing. *J. Am. Chem. Soc.* **2017**, *139*, 5067-5074.
50. Liu, N.; Lin, T.; Wu, M.; Luo, H.-K.; Huang, S.-L.; Hor, T. S. A., Suite of Organoplatinum(II) Triangular Metallaprism: Aggregation-Induced Emission and Coordination Sequence Induced Emission Tuning. *J. Am. Chem. Soc.* **2019**, *141*, 9448-9452.
51. Yan, X.; Wei, P.; Liu, Y.; Wang, M.; Chen, C.; Zhao, J.; Li, G.; Saha, M. L.; Zhou, Z.; An, Z.; Li, X.; Stang, P. J., Endo- and Exo-Functionalized Tetraphenylethylene $M_{12}L_{24}$ Nanospheres: Fluorescence Emission inside a Confined Space. *J. Am. Chem. Soc.* **2019**, *141*, 9673-9679.

52. Li, Y.; An, Y.-Y.; Fan, J.-Z.; Liu, X.-X.; Li, X.; Hahn, F. E.; Wang, Y.-Y.; Han, Y.-F., Strategy for the Construction of Diverse Poly-NHC-Derived Assemblies and Their Photoinduced Transformations. *Angew. Chem. Int. Ed.* **2019**, Doi: 10.1002/anie.201912322.
53. Yu, G.; Zhang, M.; Saha, M. L.; Mao, Z.; Chen, J.; Yao, Y.; Zhou, Z.; Liu, Y.; Gao, C.; Huang, F.; Chen, X.; Stang, P. J., Antitumor Activity of a Unique Polymer That Incorporates a Fluorescent Self-Assembled Metallacycle. *J. Am. Chem. Soc.* **2017**, *139*, 15940-15949.
54. Hofmeier, H.; Schubert, U. S., Recent developments in the supramolecular chemistry of terpyridine-metal complexes. *Chem. Soc. Rev.* **2004**, *33*, 373-399.
55. Chakraborty, S.; Newkome, G. R., Terpyridine-based metallosupramolecular constructs: tailored monomers to precise 2D-motifs and 3D-metallocages. *Chem. Soc. Rev.* **2018**, *47*, 3991-4016.
56. Wang, J.-L.; Li, X.; Lu, X.; Hsieh, I. F.; Cao, Y.; Moorefield, C. N.; Wesdemiotis, C.; Cheng, S. Z. D.; Newkome, G. R., Stoichiometric Self-Assembly of Shape-Persistent 2D Complexes: A Facile Route to a Symmetric Supramacromolecular Spoked Wheel. *J. Am. Chem. Soc.* **2011**, *133*, 11450-11453.
57. Liu, D.; Chen, M.; Li, Y.; Shen, Y.; Huang, J.; Yang, X.; Jiang, Z.; Li, X.; Newkome, G. R.; Wang, P., Vertical Assembly of Giant Double- and Triple-Decker Spoked Wheel Supramolecular Structures. *Angew. Chem. Int. Ed.* **2018**, *57*, 14116-14120.
58. Wild, A.; Winter, A.; Schlütter, F.; Schubert, U. S., Advances in the field of π -conjugated 2,2':6',2''-terpyridines. *Chem. Soc. Rev.* **2011**, *40*, 1459-1511.
59. Wang, X.-y.; Del Guerzo, A.; Schmehl, R. H., Preferential solvation of an ILCT excited state in bis(terpyridine-phenylene-vinylene) Zn(II) complexes. *Chem. Commun.* **2002**, 2344-2345.
60. Reichardt, C., Solvatochromic Dyes as Solvent Polarity Indicators. *Chem. Rev.* **1994**, *94*, 2319-2358.
61. Thomas, S. W.; Joly, G. D.; Swager, T. M., Chemical Sensors Based on Amplifying Fluorescent Conjugated Polymers. *Chem. Rev.* **2007**, *107*, 1339-1386.
62. Jakubiak, R.; Collison, C. J.; Wan, W. C.; Rothberg, L. J.; Hsieh, B. R., Aggregation Quenching of Luminescence in Electroluminescent Conjugated Polymers. *J. Phys. Chem. A* **1999**, *103*, 2394-2398.
63. Hong, Y.; Lam, J. W. Y.; Tang, B. Z., Aggregation-induced emission: phenomenon, mechanism and applications. *Chem. Commun.* **2009**, 4332-4353.
64. Yin, G.-Q.; Wang, H.; Wang, X.-Q.; Song, B.; Chen, L.-J.; Wang, L.; Hao, X.-Q.; Yang, H.-B.; Li, X., Self-assembly of emissive supramolecular rosettes with increasing complexity using multitopic terpyridine ligands. *Nat. Commun.* **2018**, *9*, 567.
65. Chan, M. H.-Y.; Ng, M.; Leung, S. Y.-L.; Lam, W. H.; Yam, V. W.-W., Synthesis of Luminescent Platinum(II) 2,6-Bis(N-dodecylbenzimidazol-2'-yl)pyridine Foldamers and Their Supramolecular Assembly and Metallogel Formation. *J. Am. Chem. Soc.* **2017**, *139*, 8639-8645.

A Giant Truncated Metallo-tetrahedron with Unexpected Supramolecular Aggregation Induced Emission Enhancement

